Supplement of The Cryosphere, 18, 819–836, 2024
https://doi.org/10.5194/tc-18-819-2024-supplement

The Cryosphere
Open Access

Supplement of

Partial melting in polycrystalline ice: pathways identified in 3D neutron tomographic images

Christopher J. L. Wilson et al.

Correspondence to: Christopher J. L. Wilson (chris.wilson@monash.edu)

Supplementary material

Partial melting in polycrystalline ice: Pathways identified in 3D neutron tomographic images

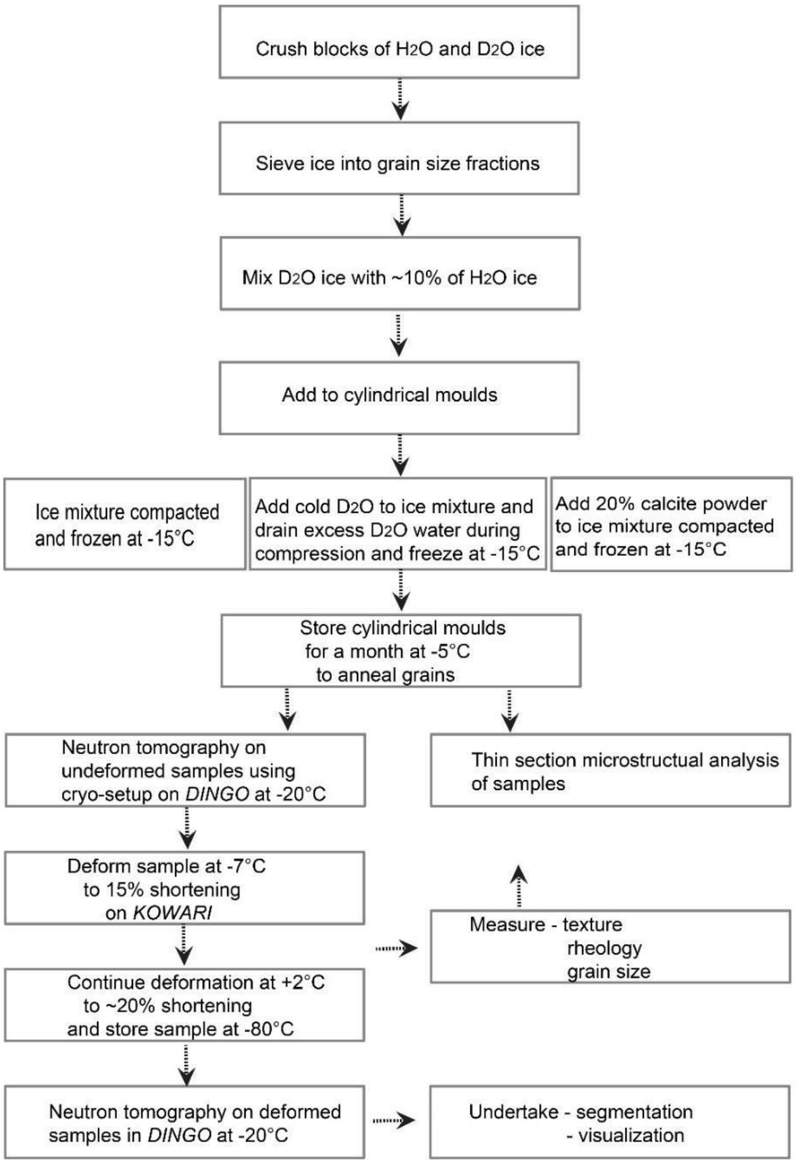

Figure S1. Schematic illustration showing workflow for 3D ice melting experiments. Involving sample preparation, deformation experiments on *KOWARI*, neutron tomography on *DINGO*, and followed by segmentation and visualization.

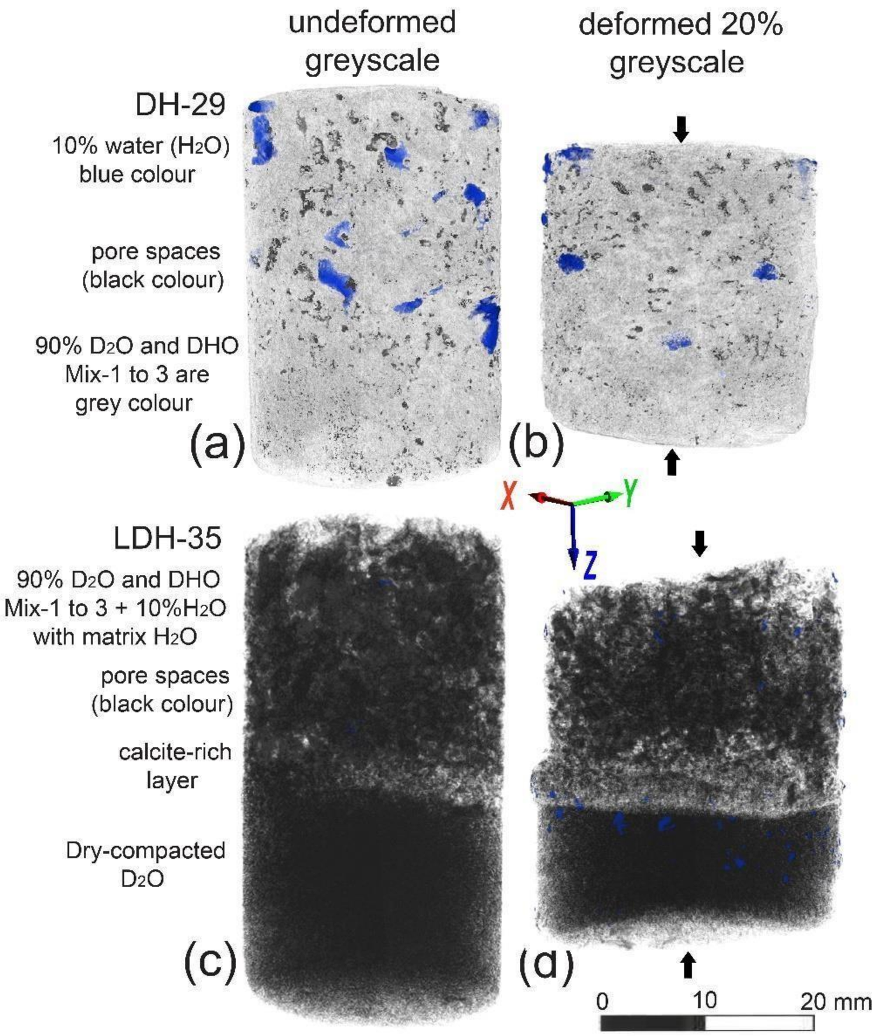

Figure S2. Illustrations of 3D tomographic images of DH-29 and LDH-35. The black arrows show the orientation of the compression in the deformed samples. (a, b) Image of DH-29 before and after deformation with location of water highlighted in blue. (c, d) Image of LDH-35 before and after deformation with layers of dry compacted and matrix filled D_2O + H_2O ice, calcite-rich D_2O ice. Water can be identified as small blue grains. In undeformed samples such as DH29 the greyscale image of the 3D surface of the cylindrical sample illustrates an irregular distribution of water (Figure S2a, blue areas) in the upper portion of the sample. After deformation (Figure S2b) water appears as elongate concentrations adjacent to the end faces of the sample, in an XY-plane, adjacent to where the piston was in contact with the sample (Figure S2b, at the top) or adjacent to inherited calcite-rich layers (Figure S2d).

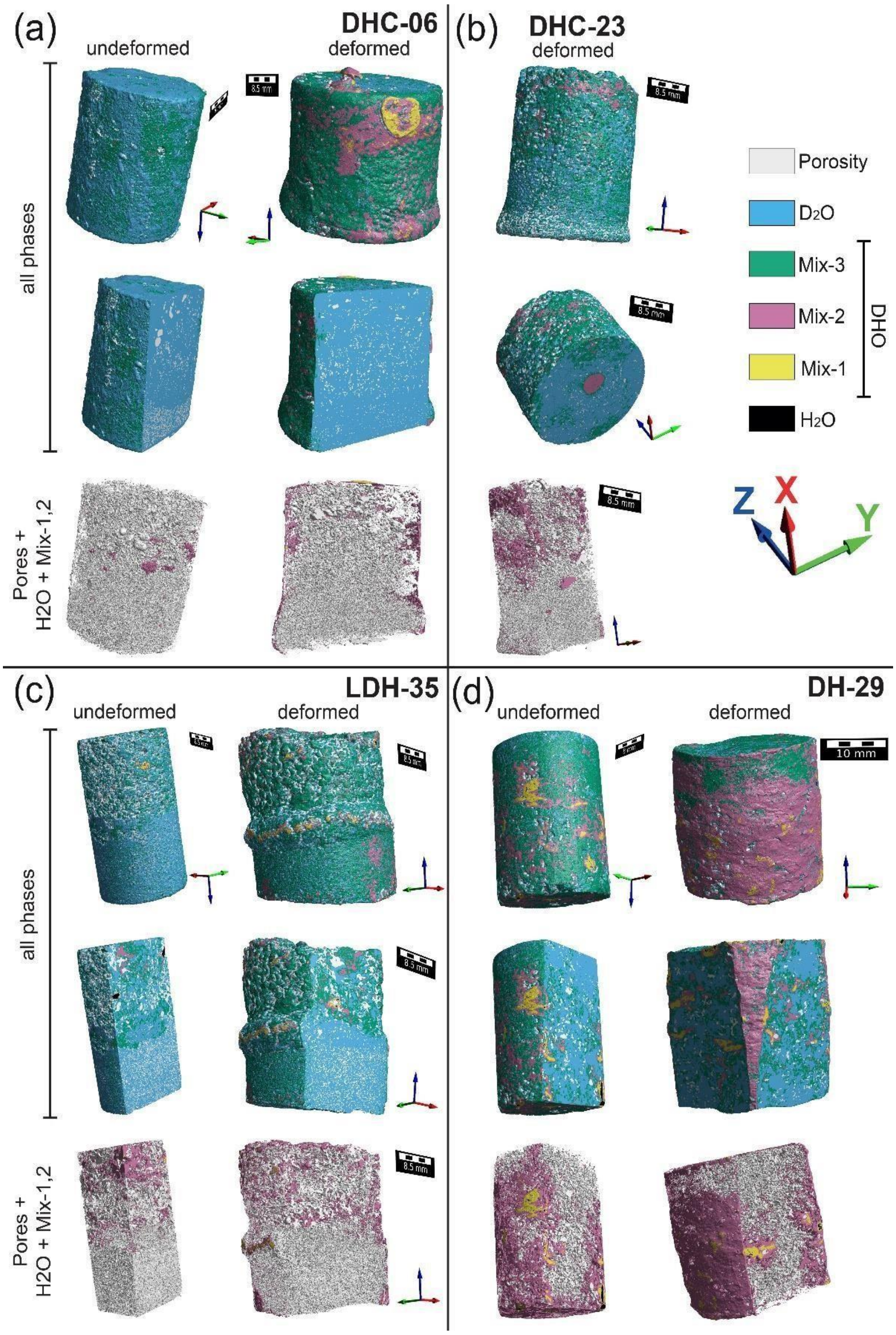

Figure S3. Illustrations of phase-labelled 3D tomographic images of DHC-06 (a), -23 (b), LDH-35 (c) and DH-29 (d). 3D surface rendering of undeformed and deformed samples (first row) + cut off (second row) of all labelled phases. In the third row, 3D rendered surface of the pores and the labelled phases H_2O, Mix-1 and Mix-2 before and after deformation are shown.

Figures S4–S6 have been uploaded as separate movies.

They are now online and the DOIs are as follows.

DOI	Title
https://doi.org/10.5446/63238	Figure S6.
https://doi.org/10.5446/63237	Figure S5.
https://doi.org/10.5446/63236	Figure S4

Figure S4. https://doi.org/10.5446/63236

3D tomographic image of deformed DHC-23 layered sample with D_2O matrix-supported layer on top of dry-compacted layer. The image illustrates the complex distribution of the pore network, Mix-2 (pink) and water (black) highlighted in YZ slices moving through the sample. With a notable Mix-2 concentration on interface between layers.

Figure S5. https://doi.org/10.5446/63237

3D tomographic image of DH-29 showing H_2O distribution after 20% shortening. The initial undeformed sample had 10% H_2O uniformly distributed within a D_2O matrix. After deformation only ~8% H_2O remains and this has moved to outer extremity of the sample. There is a complete absence of H_2O from the centre of the deformed sample.

Figure S6. https://doi.org/10.5446/63238

3D tomographic image of DH-29 showing pore distribution after 20% shortening. Pores are retained in the central portion of the sample with a minor loss adjacent to edges. There is also an increase in pore size with a slight elongation in the plane of flattening (XY). This is unlike the redistribution and loss of H_2O during the same deformation (see Figure S5).

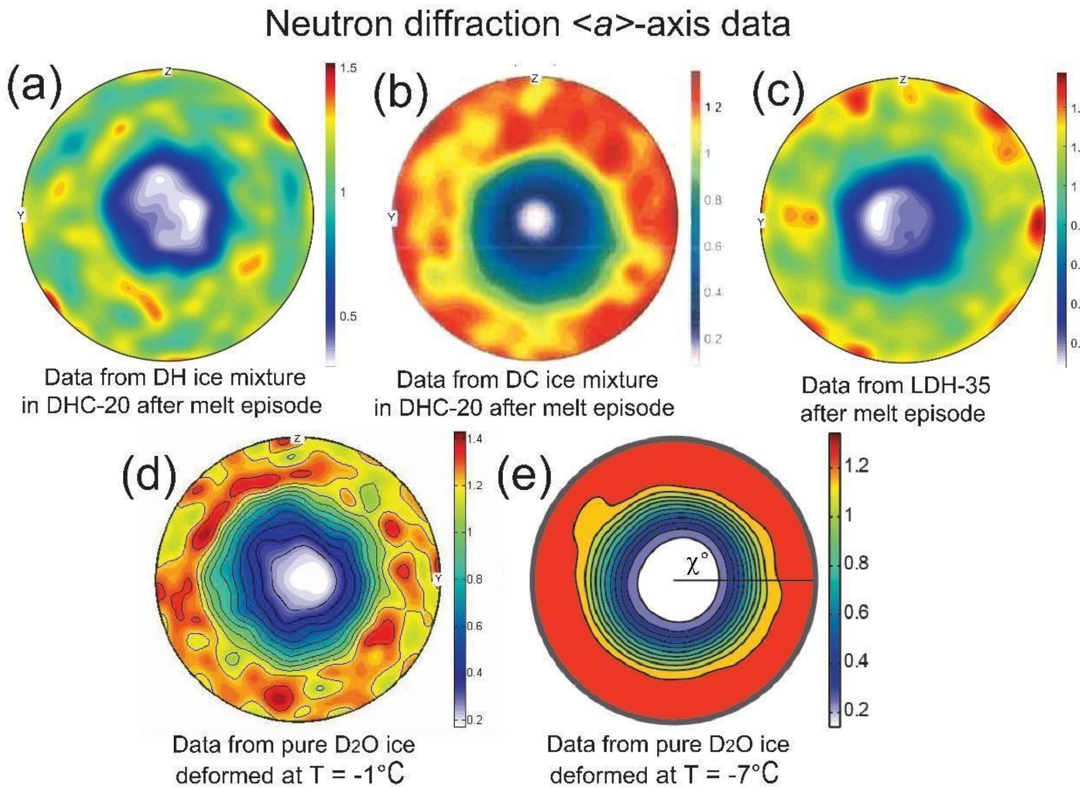

Figure S7. Representative <a>-axis neutron diffraction pole figures. Minima and maxima of density are indicated to the right of each pole figure, which are lower hemisphere, equal area projections. (a – c) Pole figures obtained from DHC-20 and LDH-35, which are weaker than the at -7 and at -1 ºC fabrics. (d) Pole figures for D1-1 deformed at -1 ºC (Table 1) showing a very good symmetrical cone around the centre of the pole figure corresponding to compression axis (X). (e) Pole figures for D1_7 deformed at -7 ºC (Table 1) showing a cluster of [c]-axes around the centre of the pole figure corresponding to compression axis (X). The polar angle χ is the angle between the compression axis (χ = 0°) and the maximum contour for the [c]-axes.